Journal of Structural Geology, Vol. 7, No. 1, pp. 45 to 56, 1985
Printed in Great Britain

0191-8141/85 $03.00 + 0.00
Pergamon Press Ltd.

Microscopic deformation mechanisms associated with mica film formation in cleaved psammitic rocks

WILLIAM J. GREGG

Department of Geology and Geological Engineering, Michigan Technological University, Houghton, MI 49931, U.S.A.

(*Received* 5 *December* 1983; *accepted in revised form* 4 *July* 1984)

Abstract—At Islesboro, Maine, cleavage is well developed in low greenschist-facies siltstones and interbedded pelites of early Paleozoic age. The siltstones contain a spatial sequence of mica film structures that corresponds to increasing intensity of mesoscopic cleavage. In the most weakly foliated rocks, cleavage is defined by the preferred orientation of individual mica particles. In siltstones displaying slightly higher strain, these particles are accompanied by short, discontinuous mica film segments, thought to have formed by the recrystallization of early pore-space layer silicates. In moderately cleaved rocks, these segments link up to form lengthened mica films by a process thought to include intergranular fracture, transgranular fracture and layer silicate crystallization. In strongly cleaved rocks, the lengthened mica films become longer and thicken appreciably by solution transfer of quartz and residual accumulation of layer silicates and opaque minerals. Layer silicate crystallization is evident at all stages of mica film development, but is especially marked by the growth of decussate mica inside late-stage, thick mica-rich layers. This sequence of mica film development is probably characteristic of fine-grained psammitic rocks, and may not necessarily occur in carbonate-rich or mica-rich rocks.

INTRODUCTION

THE DOMAINAL microscopic structure of cleavage in pelitic and psammitic rocks is typically marked by the presence of mica films (Voll 1960). Mica films are thin parallel or anastamosing seams of oriented mica particles that trend parallel to or are symmetrically inclined (Powell 1982) to the trace of mesoscopic cleavage. Despite their common occurrence there have been few attempts to define the morphology and development of these films. They are, however, an important 'building block' in the formation of mesoscopic cleavage structures and their study can offer insights into larger scale problems, such as the relationship between a developing foliation and successive incremental principal planes of strain (Means 1975). The work presented here focuses on the morphology of mica films in natural siltstones and the mechanisms operating during various stages of their development. The specimens were collected from the Island of Islesboro, Maine, U.S.A. at a northern promontory called Turtle Head (Fig. 1). They are part of the early Paleozoic Islesboro Formation of metasedimentary rocks that, together with a few small bodies of Precambrian rocks, comprises the Islesboro block. This structural block is bounded by right lateral strike-slip faults that separate simply deformed low greenschist-facies Islesboro rocks from the high grade, polyphase deformed rocks of the mainland (Stewart 1974).

SEDIMENTARY AND DIAGENETIC SETTING

Mesoscopic bedding

The portion of the Islesboro Formation that outcrops at Turtle Head is a sequence of siltstones and dark silty shales. The siltstones consist of white, finely cross-laminated beds ranging from 5 to 20 cm thick, with sharp basal and gradational upper contacts. Pelitic intervals between these beds are typically less than 5 cm thick and consist of either dark silty shale or thin pelite beds with siltstone laminae less than 1 mm thick.

On a microscopic scale S_0 is typically a fine cross-bedding marked by thin pelitic layers of chlorite–white mica aggregates or by thin beds of heavy minerals of placer origin. These opaque-mineral layers accentuate cross-bedding and form fine marker horizons of irregularly shaped, well-sorted magnetite grains in thin section. The detail of this fine sedimentary layering can be observed even inside thick secondary mica-rich layers in highly strained rocks (Fig. 2c).

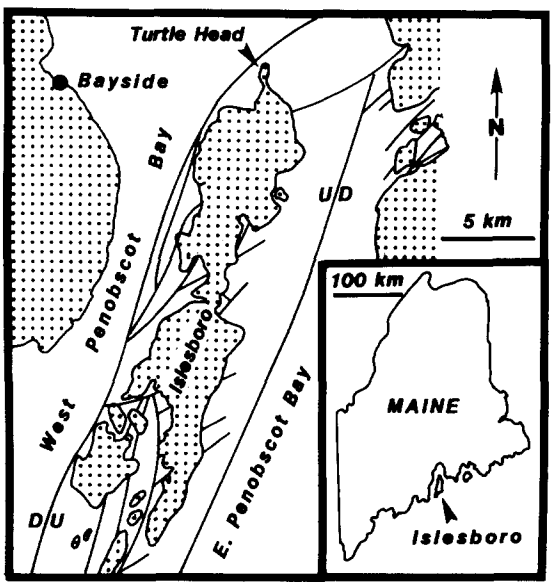

Fig. 1. Locality map. Lines indicate faults mapped by Stewart (1974).

Petrography of clastic quartz and feldspar

Universal-stage measurements show no preferred crystallographic orientation of quartz (Gregg 1979) even in the most highly strained specimens. Truncated octahedral grain shapes (Smith 1964, Hobbs 1968, Vernon 1976) and other textures associated with grain growth in quartz are absent, as are subgrains and new grains typically associated with recovery and primary recrystallization (Hobbs *et al.* 1976). Quartz grain boundaries are irregular in most cases, but straight boundaries may occur along contacts with mica grains or between well developed quartz overgrowths. Feldspar grains (An_6–An_8) are common detrital constituents and occur without obvious overgrowths. They display a fine mottled texture possibly due to sericitization.

Phi plots (Fig. 3a) made from thin-section measurements show a grain size distribution typical of moderately sorted silt-size clastic sediment (Wilson & Pittman 1977). The preservation of clastic size distribution, low metamorphic grade (Stewart 1974), lack of preferred crystallographic orientation of quartz, and absence of annealing textures suggests that quartz grain boundaries have maintained their original clastic configuration with only minor modifications due to the interlocking of quartz overgrowths into line boundaries (see also Dapples 1979).

Petrography of layer silicates

In siltstone specimens that contain no cleavage microstructures, such as those taken from the outer arcs of synformal B_1 folds, mica particles occur either as fine white mica (0.5–4 μm) or as large aggregates (20–150 μm) of interlayered white mica and chlorite. X-ray diffractometry has shown that the white mica in both cases is muscovite. The aspect ratio of the fine mica is about 4:1, and the grains are uniform in size. The fine micas are thought to be non-detrital in origin due to the absence of internal crystallographic cleavage traces, uniform extinction, and straight boundaries against adjacent minerals shown by these grains (McDowell & Elders 1980).

In areas that lack fine-scale cleavage these fine micas are statistically parallel to bedding and a minimum orientation occurs in the direction of the fold axial plane. In all other areas, however, these micas are statistically parallel to mesoscopic cleavage, and they are integral with elementary cleavage microstructures.

The large aggregate grains of interlayered chlorite and muscovite are clearly of a different origin than the fine mica described above. These irregularly shaped aggregates are never found with (001) parallel to cleavage, except where they have been strongly deformed and rotated in regions of high strain. Crystallographic cleavage traces are readily apparent in the internal chlorite layers but not usually in the muscovite layers (see Williams 1972, fig. 6). The chlorite layers around the white mica exhibit free-growth crystal shapes (Spry 1969, p. 153) and some aggregates have incorporated a number of clastic quartz and feldspar grains during growth. In rocks that contain thick cleavage domains the chlorite–white mica ratio is lowest in grains that are closest to the domains. Aggregates that have been incorporated within the domain boundaries are entirely altered to muscovite. In addition to changes in the chlorite–white mica ratio, aggregates near S_1 cleavage domains become severely distorted and display rotation of (001) away from bedding.

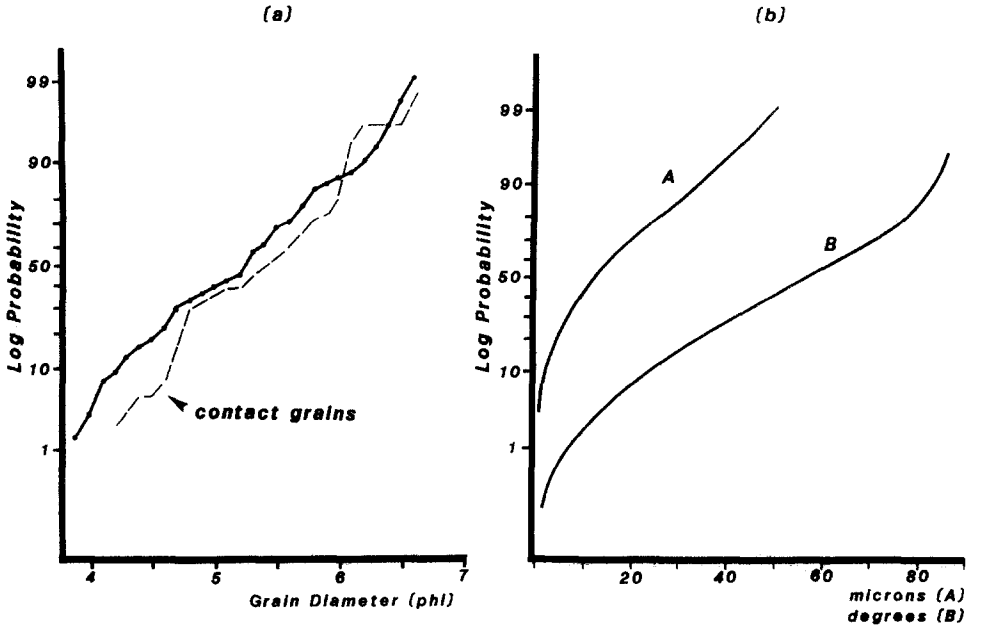

Fig. 3. (a) Phi plots for typical Islesboro siltstone grains (solid line) and grains in contact with mica film boundaries (dashed line) illustrating reduction in grain size. (b) Curve A shows probability of grain size differences between adjacent grains in undeformed siltstone. Curve B shows probability of quartz *c*-axis angular differences between adjacent grains in a randomly oriented aggregate.

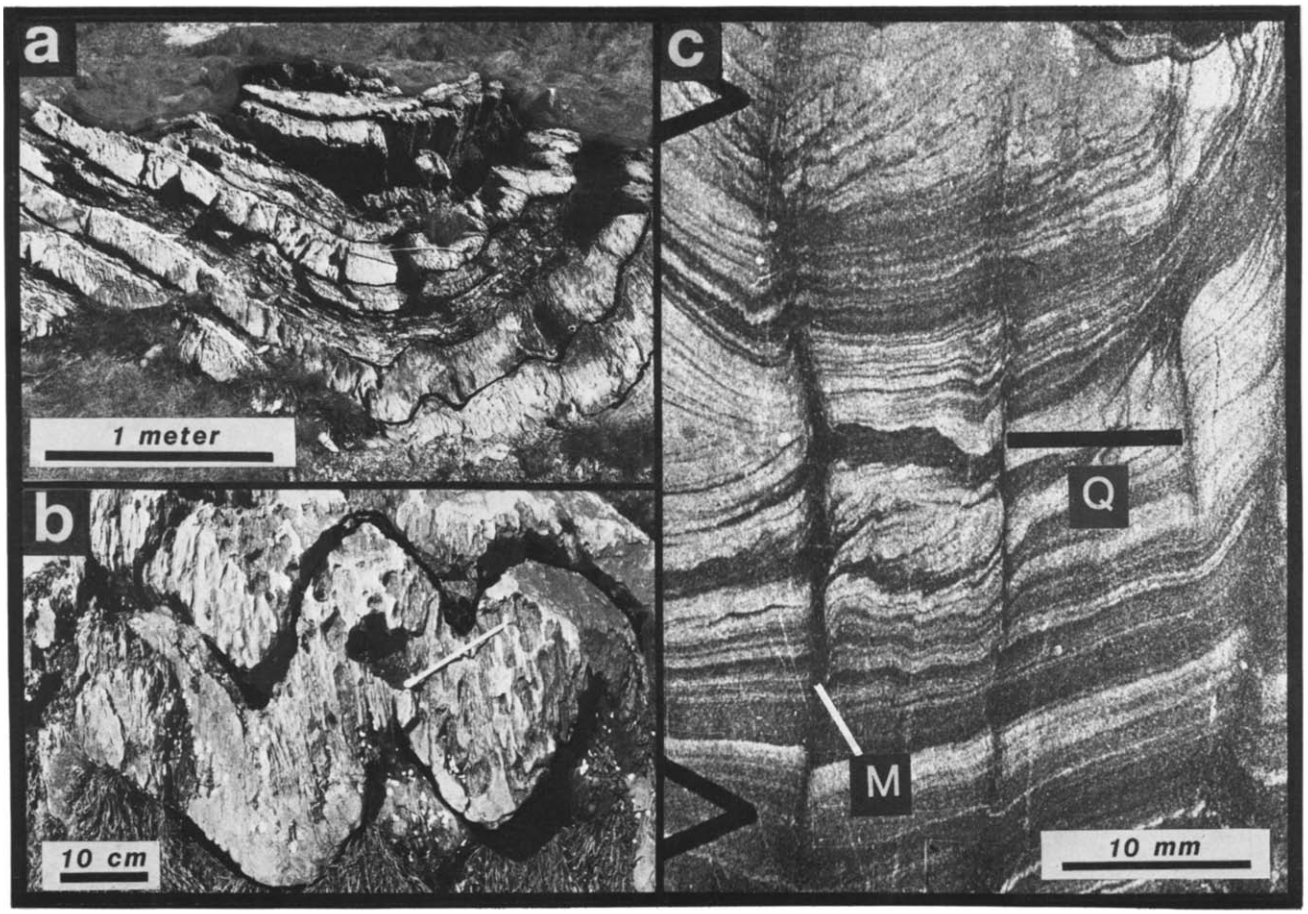

Fig. 2. Profile-plane views of B_1 folds at Turtle Head in interbedded siltstone and pelite (a) and thick siltstone beds (b). (c) Fine-scale sedimentary layering in interbedded siltstone and pelite with thick S_1 secondary layers (M-domains). Q-domains contain a weaker mica-film S_1 foliation.

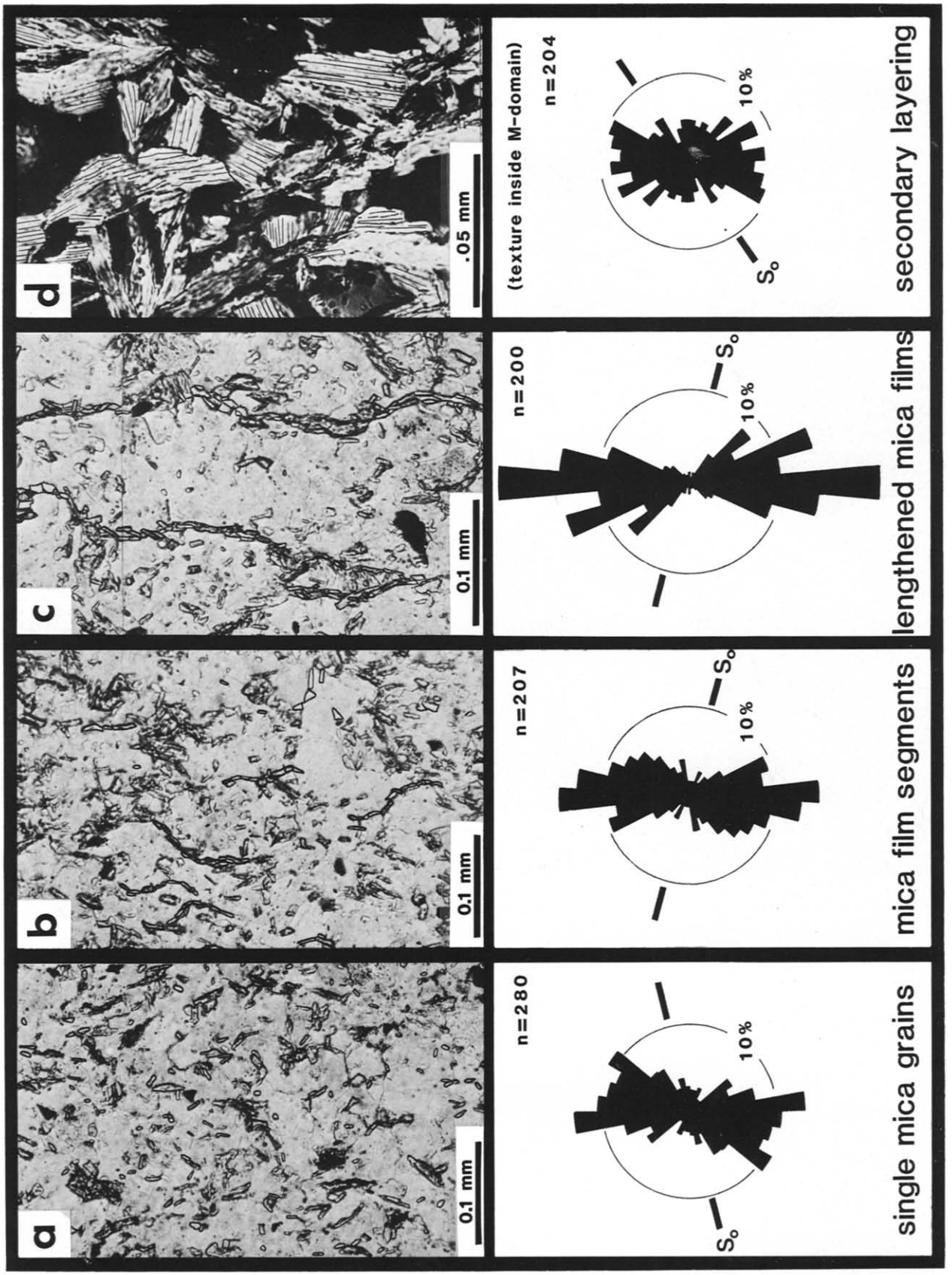

Fig. 4. (a)–(c) Photomicrographs showing spatial sequence of mica film structures, and corresponding preferred orientation of fine white mica. (d) Shows decussate mica inside a thick *M*-domain under cross-Nicols. See text for details. S_0, bedding.

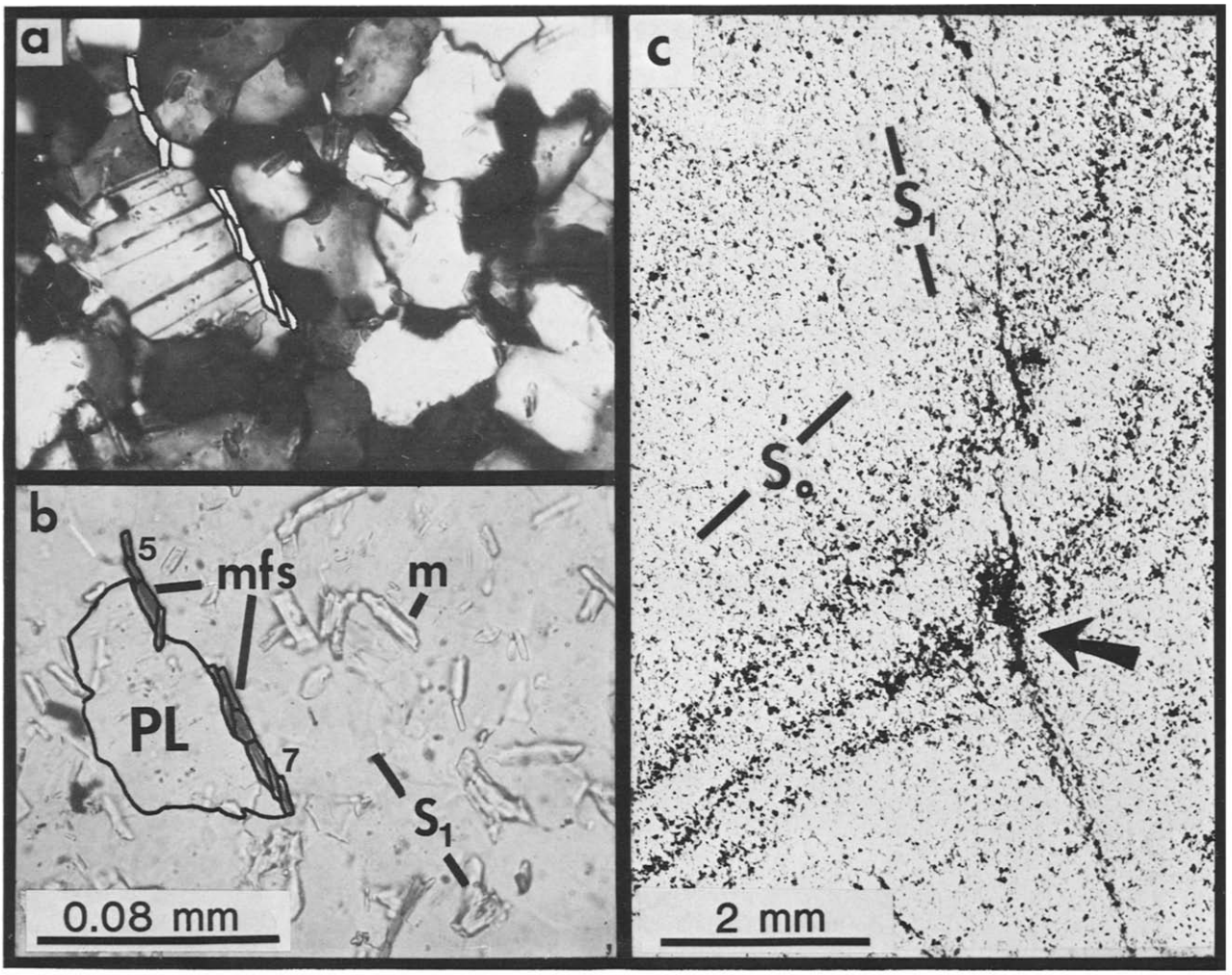

Fig. 5. (a) and (b) Mica film segment (mfs) located adjacent to a large clastic feldspar grain (PL) illustrating the typical relationship between grain boundary length and film segment length. Other layer silicates are poorly oriented but a few such as (m) are parallel to the mesoscopic trace of S_1. (c) Accumulation of opaque grains at the intersection of magnetite-rich cross beds with S_1 cleavage in siltstone.

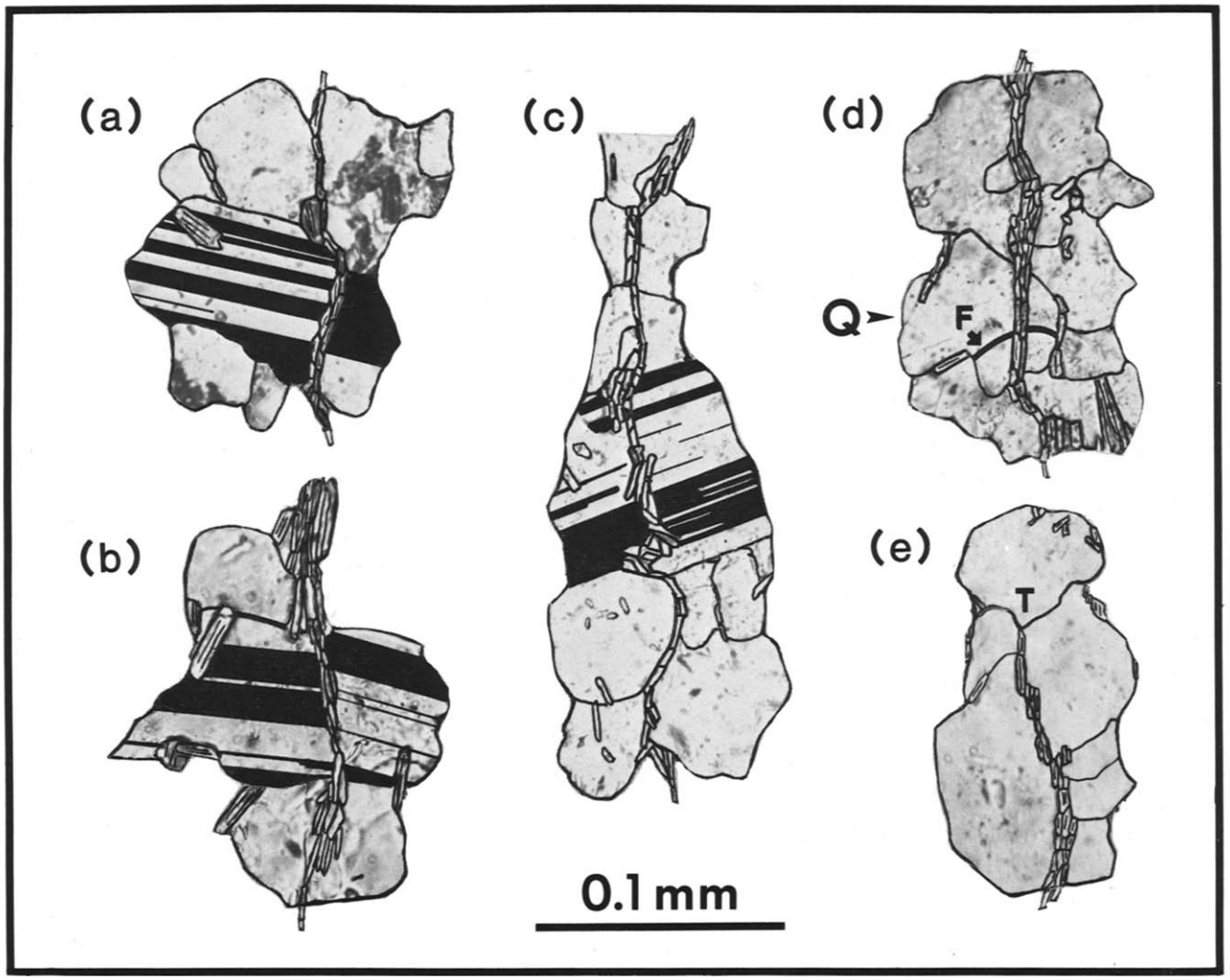

Fig. 7. (a)–(c) Photomicrographs of plagioclase grains cut into two segments by lengthened mica films. Grain (b) occurs along the mica film illustrated in Fig. 6. (d) Quartz grain cut by mica film, with early curved fracture visible on both sides of the film at F. (e) Termination, T, of a mica film segment on an adjacent quartz grain boundary.

The texture displayed by these grains suggest that the chlorite component in the aggregate was not introduced but rather destroyed by prograde metamorphism accompanying the deformation. Inside undeformed aggregates the white mica layers are infrequent, of aspect ratio up to 10:1, and parallel to bedding. They show sharp extinction under crossed Nicols, display no crystallographic cleavage traces, and are compositionally compatible with the low greenschist metamorphic grade (Stewart 1974). Bending, kinking or fraying of the muscovite was not obseved except where the entire aggregate lies within a thick mica-rich S_1 domain. These observations suggest a non-detrital origin for the layers, although the chlorite–white mica aggregates are as a whole obviously pre-cleavage in origin.

STRUCTURAL SETTING

Folds

Folds exposed at Turtle Head have been divided into two generations on the basis of overprinting relationships (Gregg 1979). B_1 folds are the most prominent structures and consist of upward-facing folds with nearly vertical axial surfaces and axes plunging 45 to N39°E (Fig. 2a). Small-scale B_1 folds are open to close folds in sedimentary layering with well developed S_1 cleavage (Fig. 2b). B_2 folds are rare steeply plunging kink folds of left-lateral symmetry. In siltstone beds they are usually developed only in S_1 cleavage, because the kink-band boundaries typically lie parallel to bedding. The width of the kink bands rarely exceeds 10 cm and individual kinks are spaced tens of meters apart. B_2 structures have no effect on macroscopic form surfaces at Turtle Head, nor on the microstructure of the siltstones.

Mesoscopic foliations

S_1 cleavage occurs as a weakly convergent cleavage in B_1 folds. The mesoscopic appearance of S_1 varies according to lithologic setting and structural position. Pelitic rocks typically display a fine slaty cleavage whereas siltstones contain two types of S_1 foliation. In siltstones that are either weakly strained or are free of pelitic laminations, S_1 is a fine penetrative cleavage defined by mica film structures (Fig. 2b). In siltstone beds that are rich in pelitic laminae or are thinly bedded and interlayered with pelite beds of nearly equivalent thickness, microlithons that contain the first type of foliation alternate with thick mica-rich compositional layers (Fig. 2c). The width of the compositional layers varies according to rock type. They are typically less than 3 mm thick in siltstones that contain few pelitic laminations or relatively low mica content. In siltstones with more frequent pelitic laminae the secondary layers may be up to 6 mm thick. These compositional layers commonly terminate where they intersect a bed which is either purely psammitic or purely pelitic (Fig. 2c).

S_2 cleavage occurs only in pelites situated within or close to B_2 kink-band boundaries, and is never found in siltstone regardless of proximity to B_2 kink folds.

MICROSTRUCTURE OF S_1 CLEAVAGE

The study of S_1 cleavage in siltstone beds was undertaken by examining a variety of lithologically similar specimens from different structural settings. In general the most well developed cleavage occurs within the inner arcs of B_1 fold hinges, where S_1 usually takes the form of a secondary mica-rich layering. In the outer arcs of synclinal B_1 folds there are large areas that are devoid of all types of S_1 microstructure, and no cleavage is present.

If one examines siltstone specimens according to increasing mesoscopic cleavage intensity, both the degree of orientation and the concentration of mica into various mica film structures also increases. The mica structures that appear in order of increasing cleavage intensity (Fig. 4) are: (1) aligned single-grain mica particles, (2) mica film segments, (3) lengthened mica films and (4) continuous mica-rich secondary layers.

Aligned single-grain mica microstructures

In rocks which display this structure, S_1 cleavage is defined by individual mica grains aligned parallel to the mesoscopic cleavage trace (Fig. 4a). The majority of the mica grains are not in aligned contact with other mica grains, so that mica films are generally absent. The rock fabric is defined by this arrangement of mica particles superimposed upon the primary quartz–feldspar texture previously described. Foliations defined exclusively by aligned single mica grains occur only in weakly strained rocks or in moderately strained rocks with low mica content. In highly strained rocks aligned single mica grains are often accompanied by more complex mica film structures. The transition from single grain to mica film dominated fabrics can be observed in individual specimens. In specimens that completely lack an S_1 cleavage, as in the case of portions of the outer arc of synclinal B_1 folds, there are no cleavage-aligned mica particles nor are there any other microscopic S_1 elements. Instead all fine white mica grains are oriented parallel to bedding.

Mica film segments

Mica film segments are short white mica films typically 1 grain (0.5 μm) thick and less than 80 μm long (Fig. 4b). The length of a mica film segment often corresponds to the dimension of a neighboring large detrital quartz or feldspar grain, as measured roughly in the direction of mesoscopic cleavage (Figs. 5a & b). This relationship gives the impression that the segments occupy areas that were initially clay or mica-filled interstices formed during deposition.

Mica film segments are the most rudimentary form of mica film structures that have been observed in these

siltstones. They are best observed in weakly cleaved specimens in which more extensive mica films are absent. In these specimens they are typically associated with aligned single mica grains (Figs. 5a & b). The presence of the segments in such examples is associated with a higher preferred orientation of fine white mica in the mesoscopic cleavage direction than is found in specimens that contain only cleavage-aligned single mica grains (compare Figs. 4a & b).

Lengthened mica films

Lengthened mica films in moderately deformed siltstones are long, planar white mica films typically 2–3 mica grains thick and commonly many tens of grains in length (Fig. 4c). Unlike mica film segments there is no relationship between the length of the film and sedimentary grain size. The length of the film may be limited, however, by bedding thickness because many films terminate gradually near bedding contacts. Mica particles within the film are typically parallel to the film length, and the boundaries of the films are sharp but not perfectly planar. The morphology of the films is the same irrespective of whether thin sections are cut orthogonal to the axial surface foliation or parallel to the cleavage-bedding intersection lineation.

Specimens that contain lengthened mica films also contain mica film segments and aligned mica particles (Fig. 4c). In some cases, mica film segments lie directly along 'strike' of, but separate from, the termination points of lengthened films. Lengthened mica films commonly braid into a series of thinner films similar in morphology to mica film segments.

Lengthened mica films in highly deformed rocks are thicker (up to 5 or 6 mica grains thick) and extend up to 10 mm in length. Examples of such thick films show a larger grain size in the internal mica, and in a few cases decussate micas are present in the film. Accumulations of opaque minerals are also found in such thick films, especially where thin sedimentary beds rich in heavy minerals are intersected by the mica film (Fig. 5c). The opaque minerals appear to have been concentrated as a solution transfer residuum. Opaque minerals inside the mica film have the same grain size and irregular grain shape as those outside the film, and thus do not appear to have been altered during residual accumulation. Thicker mica films typically contain more residual opaque material inside the mica film, thus indicating more pronounced effects of solution transfer along mica film boundaries. Similar accumulations of opaque substance in cleavage planes have been reported in many slates (e.g. Weber 1976).

Continuous mica-rich secondary layering

The most highly deformed siltstones at Turtle Head display a thick mesoscopic S_1 secondary layering. In pure siltstone beds less than 20 cm thick the secondary layers are less than 3 mm thick, but in siltstones that contain abundant pelitic laminae the secondary layers may be up to 6 mm thick (Fig. 2c). The layers are typically spaced from 5 to 20 mm apart and they display slight curvature along their length. They are much longer than all types of mica films, and range from 15 mm to many tens of cm in length. In hand specimens, secondary layers usually persist through siltstone beds that contain numerous pelitic laminae, but when the layers enter a purely psammitic or purely pelitic bed they often terminate (Fig. 2c). Thick secondary layering has not been observed in pure pelite beds or in siltstone beds that are over 20 cm thick.

On a microscopic scale, S_1 secondary layering consists of spaced compositional mica-rich layers (*M*-domains in Fig. 2c). These domains alternate with microlithons of siltstone that contain a much weaker foliation characterized by the mica film structures previously described (*Q*-domains in Fig. 2c). The boundaries of the *M*-domains vary in morphology from irregular and diffuse in the case of thinner secondary layers, to straight and abrupt in thick examples.

Inside *M*-domains, quartz and feldspar grains occur as elliptical grains or polycrystalline lenses, both of which display cleavage-parallel long axes. Secondary layers that are very thick typically contain only a few such grains and these show a higher degree of elongation parallel to cleavage compared to those in thin secondary layers. Shapes of these grains are similar to those that have been cited in the literature as indicative of corrosion (Hoeppener 1956, Williams 1972, Geiser 1974, Gray 1978, Bosworth 1981), thus they appear to be remnant clastic grains or clusters of grains that have been engulfed by the widening mica-rich layer. They display no textures indicative of recrystallization.

The main difference between *M*-domains and the lengthened mica films from which they developed is in the amount of mica contained within the domain boundaries. In the earlier stages of *M*-domain development the mica particles of the domain are of the same size and aspect ratio as those found in lengthened mica films, but this gradually gives way to an internal structure defined entirely by decussate mica. The presence of this decussate mica (Fig. 4d) within the *M*-domain results in a lower degree of preferred orientation of mica and thus reverses the trend established during the progressive growth of the mica films (Figs. 4a–c).

As previously mentioned, the trace of bedding through an *M*-domain is usually obvious both in hand specimen and thin section observation. This trace is marked by either trails of residual opaque minerals or by thin zones rich in the identifiable remnants of the large (20–150 μm) chlorite–white mica aggregates previously discussed. The opaque minerals originate from thin placer horizons in the siltstone (Fig. 5c) and the chlorite aggregates originate in pelitic laminae, where they are typically parallel to bedding. Where these chlorite–white mica aggregates become entrapped in the *M*-domain they display alteration, elongation of shape and rotation of (001) out of the bedding parallel orientation, and toward the mesoscopic trace of S_1. In the thickest *M*-domains these aggregates are completely altered to

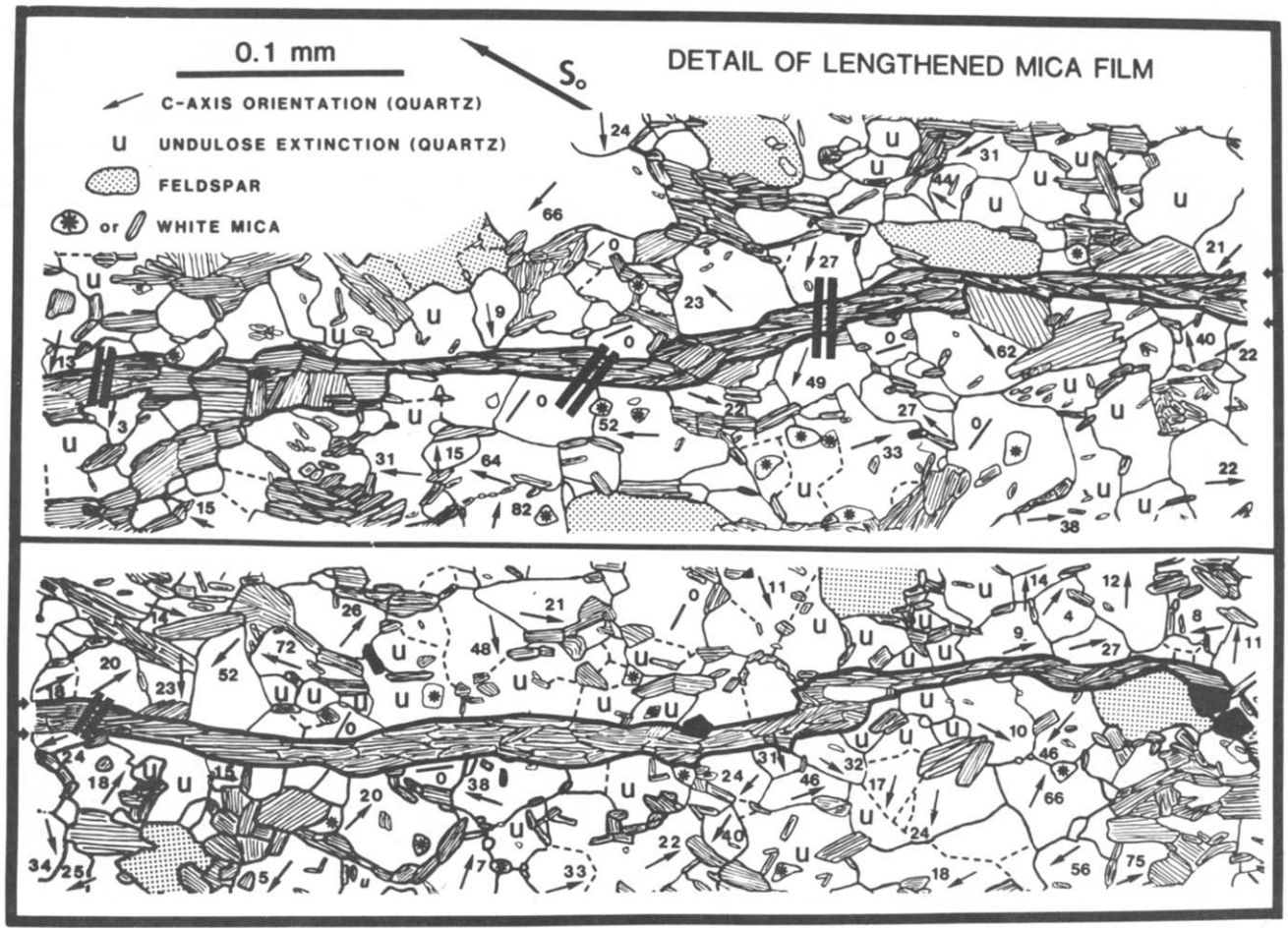

Fig. 6. 'Geologic map' of a typical lengthened mica film in cleaved siltstone. The grain size distribution of the clastic quartz and feldspar shown here is illustrated in Fig. 3(a). Map plane is normal to bedding-cleavage intersection lineation. Dashed lines represent internal fractures.

white mica, but are still distinguishable from the surrounding decussate micas by their size and shape.

EVIDENCE FOR MICROSCOPIC DEFORMATION MECHANISMS

Figure 6 illustrates the microscopic structural and mineralogical details along a portion of a typical lengthened mica film. Pelitic bedding layers containing both coarse and fine-grained micas are inclined to the film at 30°. S_0 and S_1 are steeply dipping (approximately vertical) in this view, and the plane of the map is orthogonal to the bedding cleavage intersection lineation (L_1).

The clastic quartz and feldspar grains within the quartz–feldspar domain (Fig. 6) have been classified as either 'normal' or 'contact' grains. The 'normal' grains are those that do not abut the mica film, and thus do not display effects due to mechanical or chemical processes occurring at this boundary. In the area around this mica film, 133 such grains were measured and the average grain area of the population is 840 μm^2. The word 'normal' is used to describe this population because it is assumed that the average grain size has not changed during cleavage development, compared to the 'contact' grains.

'Contact' grains are those that have a grain boundary touching the mica film. These grains typically show planar boundaries parallel to the mica film and appear truncated along the contact. There are 55 such grains in and around the area depicted in Fig. 6 and their average grain area is 605 μm^2. Compared to the 'normal' grain population, these grains show an average reduction in grain area of about 235 μm^2. Even though these two groups once belonged to the same population, the processes occurring along the mica film have resulted in statistically significant differences in their grain size distributions. Using the 'normal' group as the expected frequency distribution over six cells, and the 'contact' group as the observed frequency distribution, the value of χ^2 obtained is 46.4. Since $\chi^2_{0.005}(5) = 16.75$, the differences in grain size distribution are significant at the 0.995 confidence level. At least two mechanisms, solution transfer of quartz or intragranular fracturing, could account for this grain size reduction along the mica film.

Although evidence for solution transfer in highly developed mica films seems clear, in the form of the accumulation of opaque mineral residuum (Fig. 5c), there is also evidence for intragranular fracturing of grains as an important mechanism in the early development of films such as the one in Fig. 6. Quartz and feldspar grains that have been transected into two recognizable parts along lengthened mica films are relatively

common in these specimens (Fig. 7). This is to be expected if the mica films are to propagate in the cleavage direction. Without intragranular fracture, mica films that 'strike' into large clastic grains would be 'pinned' at terminations such as that shown in Fig. 7(e), because the relative size and distribution of clastic grains with respect to the mica films does not provide a condition in which propagation could proceed entirely along clastic grain boundaries.

Where obvious internal markers such as twinning are absent, it is still possible to recognize truncated grains by the coincidence of *c*-axis orientation of the separated grain fragments. The grains marked by double lines in Fig. 6 show four such cases along the film boundary where detrital quartz grains have been cut by the mica film into two parts that have closely matching *c*-axis orientations and chord lengths (length of the contact with the mica film). From left to right in Fig. 6 the angular difference in *c*-axis orientation for each pair is 10, 32, 19 and 42°. The corresponding differences in chord length for these pairs are 9, 1, 19 and 5 μm. To determine the statistical significance of this data, comparisons were made with the angular *c*-axis difference and grain diameter differences that occur between adjacent grains as a result of normal sedimentation processes. The probability of grain size differences was assessed using the information in Fig. 3(a) and is presented as a semi-variogram (curve A in Fig. 3b). The probability of random *c*-axis angular differences was determined by a Monte Carlo method (42,000 iterations) and is plotted as curve B in Fig. 3(b). These curves were used to calculate the joint probability of chance coincidence of *c*-axes due to sedimentary processes. For the four grain pairs noted, the joint probability of chance occurrence is 0.007, 0.0010, 0.001 and 0.0675, respectively. In addition to these grain pairs, the plagioclase grain that is bisected in Fig. 7(b) occurs along strike of the same mica film illustrated in Fig. 6.

Besides supporting the role of intragranular fracture in the early development of mica films, these grain pairs provide a crude limit on the amount of material that could have been removed by solution transfer along the film boundaries at this stage. Given the average grain size of the undeformed silt grains, the removal of more than 25 μm of material along the film by solution transfer would result in fewer than four matching grain pairs due to complete dissolution of the remains of other matching pairs. Using 25 μm as an upper limit of quartz grain solution transfer, therefore, and given a mica content from 21 to 29%, the resulting residual mica film would be about 5 or 8 μm thick.

A similar rough estimate can be made by comparing the average grain area of the 'normal' grains (840 μm^2) with the 'contact' grains (605 μm^2). This average reduction of 235 μm^2 per grain, divided by the average initial grain diameter of 32.7 μm, yields an average depth of 7.2 μm of quartz removed along both sides of the mica film. The corresponding amount of residual mica would be 3.0–4.0 μm thick based on the 21–29% mica content of the siltstone. This calculation does not take into account grain size reductions due solely to intragranular fracture along the developing mica film, thus the calculated amount of residual mica is a slight over-estimate.

The mica film thicknesses calculated by both methods are less than the actual film thickness, which averages 13 μm. Furthermore, on the basis of the known mica content of this siltstone the mica film thickness of 13 μm would require the removal of 50–65 μm of material by solution transfer. The removal of such a large amount would result in no matching grain pairs due to total dissolution of the initial contact grains. It seems likely then that residual accumulations of mica produced by solution transfer of quartz account for only about one-half of the mica film thickness in this example. The remaining mica may have been part of the original mica film segments or alternatively may have been emplaced in the film by crystallization.

The role of crystallization is clear if one considers the examples of bisected plagioclase grains shown in Fig. 7, especially example (b) which lies along the same film as in Fig. 6. Because the plagioclase grains contain no included mica particles, it would not be possible to accumulate the amount of mica in the film as an insoluble residue during solution transfer of plagioclase. Therefore the mica present in the film between both halves of the grain could only have been emplaced by crystallization, or by translation of solid mica particles, the latter being unlikely.

DISCUSSION

The work presented here concentrates on the mechanisms operating on the scale of individual cleavage domains, in rocks that are weakly cleaved and where solution transfer processes have not obliterated the evidence of early stages of development. In these rocks, penetrative cleavage has developed as a continuously evolving structure during folding. The model suggested for cleavage development is one in which mica film segments nucleate in favorable locations, link up, and are gradually extended into larger structures such as mica-rich secondary layering.

Formation of mica film segments

The formation of mica film segments appears to be the first stage in the development of continuous mica film structures in these rocks. These segments form roughly parallel to the mesoscopic cleavage direction, along the boundaries of individual clastic grains. Segments occurring along different clastic grain boundaries are not usually interconnected at this stage, and there is no evidence of either solution transfer or fracturing along the segments. The mica grains in the segments are the same size, shape and composition as the individual cleavage-aligned micas found in weakly deformed rock, and the bedding-parallel micas in uncleaved specimens. The segments could have formed by: (1) development of minute 'solution seams' (Gray 1978) along grain bound-

aries subject to high normal stress (volume decrease along boundary); (2) crystallization of mica along clastic grain boundaries previously devoid of layer silicates (volume increase along boundary) or (3) recrystallization and reorientation of adjacent pore space layer silicates along clastic grain boundaries subject to high normal stress (no volume change along boundary). Although there is no conclusive evidence in favor of either of the other processes, the 'solution seams' origin seems unlikely in these examples because of the lack of evidence for solution transfer on the film boundaries. In these rocks, the segments do not consist of some optically unresolved mica 'residuum', but of recognizable mica particles that display no kinking, fraying or other effects that one would expect from mechanical rotation of the grains as they accumulated during the solution transfer process. The similarity of the mica in the segments to undeformed recrystallized micas that occur parallel to bedding in uncleaved rock specimens suggests that the film segment mica may also be formed from recrystallized early layer silicates. This could also account for the relationship between film segment length and clastic grain size. Furthermore, the process is compatible with Oertel's (1983) observation on the permanence of phyllosilicate sheet structures in slates. For these reasons the author favors the second hypothesis, although the evidence is not conclusive.

The solution seam origin cannot be ruled out as a possibility in other rock types, however, especially in those that contain mineral constituents more susceptible to strain solution. As Bosworth (1981) pointed out, grain boundaries that are subjected to higher normal stress would have higher dislocation densities and thus would be preferentially dissolved relative to grain boundaries under lower normal stress. Where mica film segments are beginning to form, and no continuous channelways for solution transfer exist, this corrosion would be limited by the amount of pore fluid available.

Regardless of which mechanism was responsible for the actual formation of the mica film segment, for the process to continue beyond the point of formation, linkage of segments would have to occur.

Linkage of film segments

The presence of truncated clastic grains along mica films in these rocks indicates that irrespective of whether the segments developed by recrystallization or as solution seams, transgranular fracture and grain boundary fracture are important in the linkage process (Fig. 8).

In order to develop into more continuous mica film structures mica film segments must become interconnected by the crystallization or accumulation of mica somewhere between the isolated segments. This interconnection could occur along a suitably oriented grain boundary between two large clastic grains, but if no such boundary were available the interconnection could only be achieved by fracturing through an abutting clastic grain, with subsequent crystallization of new mica in the interconnecting fracture. This fracture process would not necessarily result in slip parallel to the mica film boundary, since the deformation would occur in response to the unique stress concentrations occurring in the clastic grain at the tip of the mica film segment.

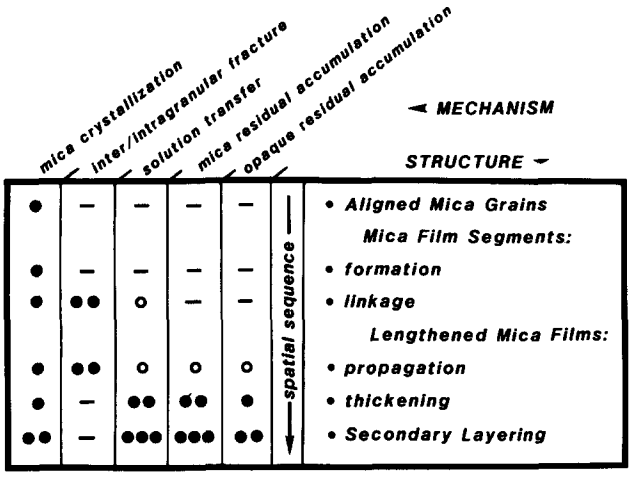

Fig. 8. Mechanisms associated with various stages of mica film development. Dashes indicate that the effects of a mechanism were not observed. Open circles indicate mechanism is present but relatively unimportant. Solid dots show relative importance of mechanism at particular stage of development.

The possible role of transgranular fracture in association with solution transfer was discussed by Elliott (1973). Gray (1978) speculated that a 'solution seam' could propagate lengthwise like a crack because of stress concentrations at the ends of the seam. Fletcher & Pollard (1981) also discussed the propagation of hypothetical 'anti cracks' due to stress concentrations at the crack tip, although they envisioned enhanced corrosion at the tip as the mechanism rather than fracture. Propagation by enhanced corrosion at the crack tip may be possible in some rock types, but the transected grains in these particular rocks do not show the usual effects of corrosion along the crack.

Many authors have commented on the general absence of clastic grains that display evidence for brittle deformation along mica film boundaries (Gray 1977), although examples of transected grains in rocks that display rough cleavage are known (Onasch 1983). The absence of such evidence is probably due to the corrosion of previously fractured grains by solution transfer. In the Islesboro rocks, evidence for transgranular fracture is common in weakly cleaved rocks, but is rare in strongly cleaved specimens that display evidence for extensive solution transfer.

Development of thick mica-rich secondary layering

In the Islesboro rocks, linkage of mica film segments is followed by the propagation and thickening of lengthened mica films. These structures propagate by the same means through which the linkage of mica film segments occur. They differ from mica film segments in that the boundaries of these films provide continuous planar cracks that act as 'channelways' for fluid migration as envisioned by Mosebach (1952) and Williams (1972).

Thus the mica films begin to thicken by the dissolution of clastic grains and the residual accumulation of layer silicates and opaque minerals along the boundaries. Early chlorite–mica aggregates display the effects of rotation, deformation and recrystallization as a consequence of their incorporation into the thickening mica-rich domains. Throughout cleavage development the degree of orientation of fine white mica steadily increases (Figs. 4a–c), but recrystallization in the thickest mica-rich domains results in the growth of decussate mica and a reduction of mica preferred orientation in the *M*-domains (Fig. 4d).

Mica films in mica-rich rocks

Structures similar to mica film segments have been reported in some weakly foliated shales. Hoeppener (1956) reported sericite layers (Serizitlagen) that progressively lengthen and thicken up to 5 μm or more as the strength of the foliation increases, in much the same way as the mica film structures at Islesboro. It seems likely then that the microstructures and mechanisms discussed here may occur in other rock types. Work done on mica-rich rocks, however, has shown a very different spatial sequence of cleavage structures (Oertel 1983). For example, White & Johnston (1981) show the development of slaty cleavage from pre-existing micro-crenulations by crystallization and solution transfer processes. Williams (1983) emphasized the role of rigid body rotation of layer silicates in the development of S_2 cleavage in deformed shale clasts, and comments that transposition of an early foliation by microfolding may be a common mechanism of cleavage development in mica-rich rocks. In both of these examples it is likely that mica film segments are formed by the recrystallization of mica parallel to axial surfaces either in both limbs of symmetric microfolds or in the long limbs of asymmetric microfolds (Marlow & Etheridge 1977, Williams *et al.* 1977). It is therefore likely that mica films develop by processes much different from those discussed here in mica-rich or carbonate-rich rocks. As Means (1975) has commented there are "slates and slates". Perhaps this also applies to mica films.

Acknowledgements—I thank Win Means for many helpful comments given during this study. I would also like to thank Paul Williams, as well as an anonymous reviewer, whose patient efforts in refereeing the manuscript for the journal improved the quality of the presentation considerably.

REFERENCES

Bosworth, W. 1981. Strain-induced preferential dissolution of halite. *Tectonophysics* **78**, 509–525.

Dapples, E. C. 1979. Diagenesis of sandstones. In: *Diagenesis in Sediments and Sedimentary Rock* (edited by Larsen, G. & Chilingar, G. V.). Elsevier, Amsterdam, 31–97.

Elliott, D. 1973. Diffusion flow laws in metamorphic rocks. *Bull. geol. Soc. Am.* **84**, 2645–2664.

Fletcher, R. C. & Pollard, D. D. 1981. Anticrack model for pressure solution surfaces. *Geology* **9**, 419–424.

Geiser, P. A. 1974. Cleavage in some sedimentary rocks of the Central Valley and Ridge Province, Maryland. *Bull. geol. Soc. Am.* **85**, 1399–1412.

Gray, D. R. 1977. Morphological classification of crenulation cleavage. *J. Geol.* **85**, 229–235.

Gray, D. R. 1978. Cleavages in deformed psammitic rocks from southeastern Australia: their nature and origin. *Bull. geol. Soc. Am.* **89**, 577–590.

Gregg, W. J. 1979. The development of foliation, in low, medium and high grade metamorphic tectonites. Unpublished Ph.D. thesis, State University of New York at Albany.

Hobbs, B. E. 1968. Recrystallization of single crystals of quartz. *Tectonophysics* **6**, 353–401.

Hobbs, B. E., Means, W. D. & Williams, P. F. 1976. *An Outline of Structural Geology*. Wiley, New York.

Hoeppener, R. 1956. Zum Problem der Bruchbildung, Schieferung und Faltung. *Geol. Rdsch.* **46**, 247–283.

Marlow, P. C. & Etheridge, M. A. 1977. Development of a layered crenulation cleavage in mica schists of the Kanmantoo Group near Macclesfield, South Australia. *Bull. geol. Soc. Am.* **88**, 873–882.

McDowell, S. D. & Elders, W. A. 1980. Authigenic layer silicate minerals in Borehole Elmore 1, Salton Sea Geothermal Field, California, U.S.A. *Contr. Miner. Petrol.* **74**, 293–310.

Means, W. D. 1975. Natural and experimental microstructures in deformed micaceous sandstones. *Bull. geol. Soc. Am.* **86**, 1221–1229.

Mosebach, R. 1952. Zur petrographie der Dachschiefer des Hünsruck-Schiefers. *Z. dt. geol. Ges.* **103**, 368–376.

Oertel, G. 1983. The relationship of strain and preferred orientation of phyllosilicate grains in rocks—a review. *Tectonophysics* **100**, 413–447.

Onasch, C. M. 1983. Dynamic analysis of rough cleavage in the Martinsburg Formation, Maryland. *J. Struct. Geol.* **5**, 73–81.

Powell, C. McA. 1982. Conjugate cleavage in quartzose sandstone (II). In: *Atlas of Deformational and Metamorphic Rock Fabrics* (edited by Bayly, B. B., Borradaile, G. J. & Powell, C. McA.). Springer, Berlin, 266–267.

Smith, C. S. 1964. Some elementary principles of polycrystalline microstructure. *Met. Rev.* **9**, 1–48.

Spry, A. 1969. *Metamorphic Textures*. Pergamon Press, Oxford.

Stewart, D. B. 1974. Precambrian rocks of Seven Hundred Acre Island and development of cleavage in the Islesboro Formation. New England Intercollegiate Geol. Conf., Guidebook for 66th Annual Meeting, 86–98.

Vernon, R. H. 1976. *Metamorphic Processes*. Allen & Unwin, London.

Voll, G. 1960. New work on petrofabrics. *Geol. J.* **2**, 503–567.

Weber, K. 1976. Gefugeuntersuchungen an transversalgeschieferten Gesteinen aus dem östlichen Rheinischen Schiefergebirge. *Geol. Jb.* **15**, 3–98.

White, S. H. & Johnston, D. C. 1981. A microstructural and microchemical study of cleavage lamellae in a slate. *J. Struct. Geol.* **3**, 279–290.

Williams, P. F. 1972. Development of metamorphic layering and cleavage in low grade metamorphic rocks at Bermagui, Australia. *Am. J. Sci.* **272**, 1–47.

Williams, P. F., Means, W. D. & Hobbs, P. E. 1977. Development of axial plane slaty cleavage and schistosity in experimental and natural materials. *Tectonophysics* **42**, 139–158.

Williams, P. F. 1983. Timing of deformation and the mechanism of cleavage development in a Newfoundland mélange. *Maritime Sediments and Atlantic Geol.* **19**, 31–48.

Wilson, M. D. & Pittman, E. D. 1977. Authigenic clays in sandstones: recognition and influence on reservoir properties and paleoenvironmental analysis. *J. sedim. Petrol.* **47**, 3–31.